33RD CONGRESS
OF THE INTERNATIONAL COUNCIL
OF THE AERONAUTICAL SCIENCES
STOCKHOLM, SWEDEN, 4-9 SEPTEMBER, 2022

ICAS 2022 SWEDEN

NON-INTRUSIVE AEROTHERMAL CHARACTERIZATION OF SURFACE HEAT EXCHANGERS FOR TURBOFAN AEROENGINES

A. Broatch[1], J. García-Tíscar[1], A. Felgueroso[1], M. Gelain[2] & A. Couilleaux[2]

[1]CMT – Motores Térmicos, Universitat Politècnica de València, Camino de Vera, 46022, Valencia, Spain
[2]Safran Aircraft Engines, Rond-point René Ravaud, 77550 Moissy-Cramayel, France

Abstract

New generations of turbofans pursue to fulfill the objectives set in Europe's FlightPath 2050 regarding fuel consumption, gas emissions, and noise generation in the aviation sector. Nevertheless, their thermal management becomes a major challenge to address, especially in terms of their oil system. For this reason, the investigation of new ways to refrigerate the lubricant is one of the major concerns during the development of these aeroengines, having the usage of Surface Air-Cooled Oil Coolers in the bypass duct been proposed as one of the possible solutions. It is however necessary to understand that preliminary investigations should be performed in reduced-scale wind tunnels to save time and costs. Despite these advantages, scaled wind tunnels suffer from an important drawback: the fact that intrusive measurements can affect the results. In this work, a methodology to characterize non-intrusively this type of heat exchanger is proposed, presenting results obtained from PIV, LDA, and LDV measurements, in addition to a pressure drop characterization, to determine the aerodynamic performance of the heat exchanger together with results measured with infrared thermography that allow deriving thermal parameters such as the Nusselt number of the heat exchanger.

Keywords: Thermal management system; Experimental aerodynamics; Wind tunnel; SACOC; SAOHE

1. Introduction

One of the key aspects of new generation aero-engines aiming to meet Europe's FlightPath 2050 goals is thermal management. Geared turbofans (GTF) and ultra-high bypass ratio (UHBR) engines can significantly reduce fuel consumption, noise, and pollutant emissions, lowering the impact of aviation on climate change. However, they require a substantial improvement of their cooling systems [1]. The main reasons for that, besides an increase in the thermal load due to the gearbox required to maintain the optimal rotation speeds of the fan and the turbine, are a rise in the core power that is transmitted to the bearing system [2] and a reduction in heat sinks [3, 4]. Furthermore, as fuel efficiency improves, less fuel can be used in Fuel-Oil Heat Exchangers (FOHEs) to provide cooling.
A promising technology to overcome this challenge is surface heat exchangers, commonly known as Surface Air-Cooled Oil Coolers (SACOCs) or Surface Air-Oil Heat Exchangers (SAOHEs), installed in the turbofan bypass [5]. These are typically finned heat exchangers which use the bypass airstream as the heat sink, which has the advantage of increasing the enthalpy budget at the bypass nozzle. However, pressure drop and flow distortion can affect the efficiency of the engine.
Therefore, these heat exchangers need to be thermo-aerodynamically characterized to determine their impact on the bypass flow versus their heat removal capacity. Furthermore, vibration analysis is also an important aspect of their design, as it is related to noise emissions and component durability. As full-scale engine tests are time-consuming and expensive, a scaled wind tunnel matching real bypass conditions has been developed at Universitat Politècnica de València in the framework of the Clean Sky 2 project "SACOC". Since reduced-scale wind tunnels can be highly sensitive to intrusive instrumentation, non-intrusive techniques such as Particle Image Velocimetry (PIV) [6, 7], Laser Doppler Anemometry (LDA) [8, 9], Laser Doppler Vibrometry (LDV) [10], and infrared thermography [11, 12] have been implemented and validated against intrusive measurements in this investigation.

2. Methodology

2.1 Facility and conceptual approach

The goal of the proposed facility is to characterize surface air-oil heat exchangers under realistic engine bypass conditions at take-off. A 500 kW two-stage radial compressor is used to deliver air at near ambient conditions to the test room. There, air enters the wind tunnel settling chamber through a pierced-radial entry that stagnates the flow. Two honeycomb meshes inside the chamber fulfill the purpose of laminating the flow and reducing turbulence levels. Then, a 12:1 contraction leads the fluid to a square section where, after a certain distance has allowed the flow to develop, a 3D printed distortion panel is affixed. This distortion panel is a honeycomb structure with variable porosity that induces a controlled total pressure drop downstream, so the developed flow inside the duct can be rearranged into the desired velocity distribution. The objective is to reproduce the boundary layer that the heat exchanger will find in the actual bypass of the engine, as depicted in Fig. 1.

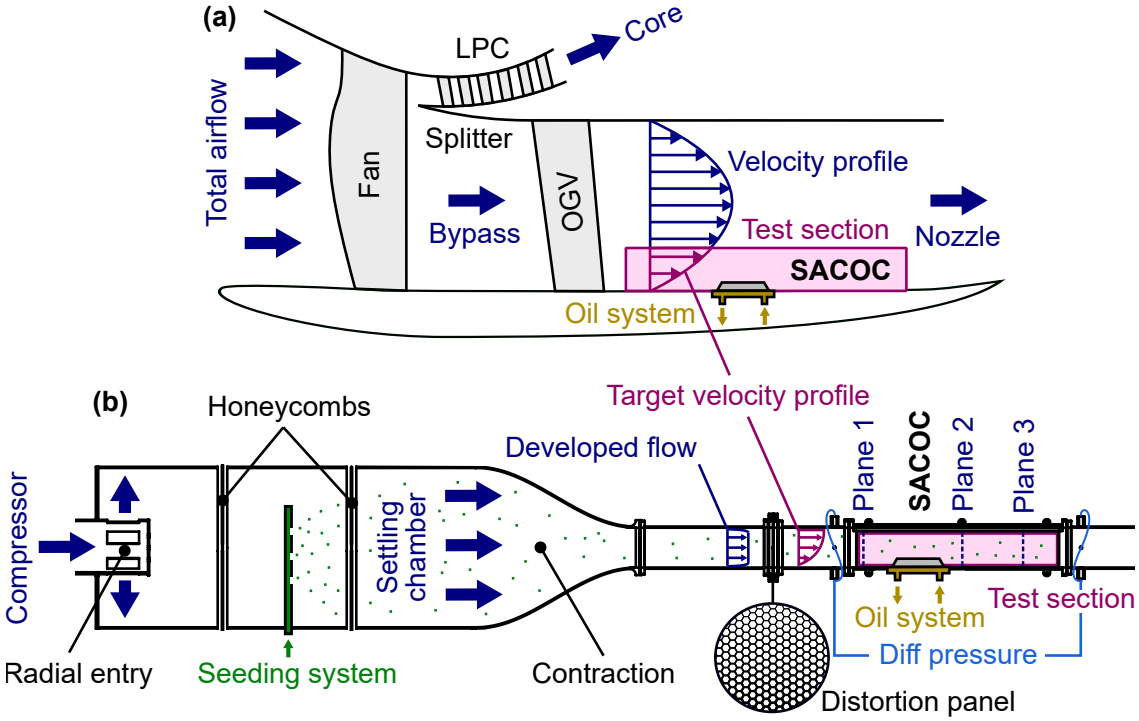

Figure 1 – Conceptual approach: (a) SACOC in the actual engine, (b) reduced-scale wind tunnel.

After the panel, the air reaches the test section where the finned heat exchanger is connected to an oil conditioning system. The lateral and top walls of the test section are made of borosilicate, specially treated for transparency to laser wavelengths. Since it is modular, the top wall can be substituted by another one that allows performing intrusive measurements in three planes: one upstream of the SACOC, and two downstream.

The oil conditioning system is composed of a pump, a series of filters and water heat exchangers, a Coriolis mass flow meter, two in-series resistors, and a PID control system that delivers the required power to the resistors to maintain a specific oil temperature. To enhance the heat exchange, two aspects have been considered: on the one hand, the heat exchanger features a series of parallel fins similarly to the air side and, on the other hand, the oil flows in counter current, i.e., in the direction opposite to the air.

2.2 Instrumentation

On the air side, the aerodynamic characterization has been performed with techniques such as high-speed PIV and LDA, carrying out also LDV measurements for fin vibration analysis. The material of the test section was specifically selected for improved transparency at the wavelengths of the different laser systems. Figure 2 shows the facility with different types of measurement setups.

2.2.1 Laser velocimetry techniques: PIV & LDA

The PIV system is a Dantec Dynamics apparatus consisting of an LD30-527 Litron laser, a Phantom VEO 640 high-speed camera, and a BNC 575 pulse generator. Regarding the laser source, it is produced by two CW-pumped Q-switched Nd:YLF DPSS laser resonators, their beams being redirected through a series of mirrors into an optic device made up of three lenses that convert the entering beam into a laser sheet. The Phantom camera, with an acquisition frequency of 1.4 kHz at maximum resolution (4 MPx), is equipped with a Zeiss Planar T*1.4/50 mm ZF.2 lens, and a green filter for 532$\pm$5 nm wavelengths. Both devices are synchronized via the pulse generator, which triggers TTL pulses with a defined delay through independent channels. Results have been obtained after averaging sets of 3000 pairs of images acquired at 1 kHz with a time delay between pulses of 10 μs. The adaptive processing varies the interrogation window between 64 $\times$ 64 and 32 $\times$ 32 pixels, using also peak ratio validation and neighbourhood outlier detection procedures.

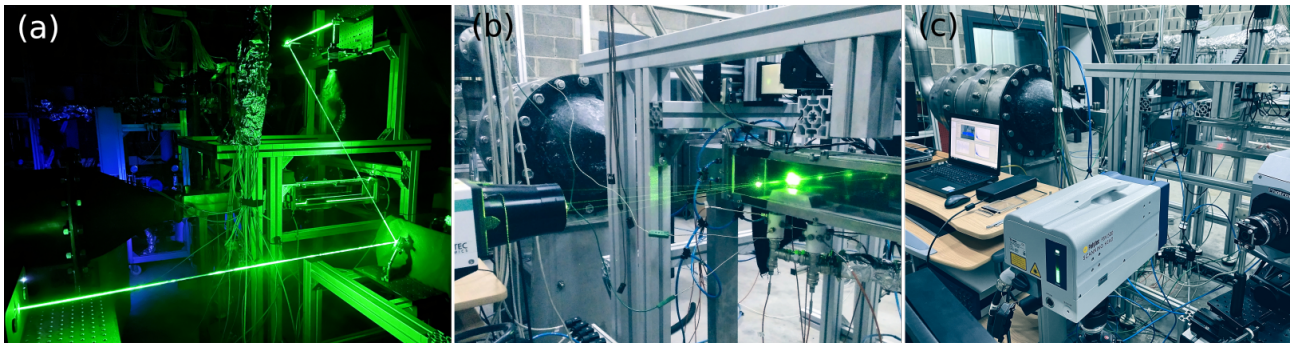

Figure 2 – The wind tunnel during non-intrusive measurements: (a) PIV, (b) LDA and (c) LDV.

Laser Doppler Anemometry measurements have been performed with a Dantec FlowExplorer DPSS 500 2D with an optic lens of 64 mm diameter and 500 mm focal length, mounted on an automated XYZ gantry. Since it emits two pairs of laser beams, one with a wavelength of 532 nm and another one of 561 nm, perpendicular to each other, two velocity components can be derived. The polarization of the beams is normal to the plane they form, allowing both pairs to intersect in the same spot without interfering with each other. An 80 MHz Bragg cell is used to generate the second beam of each pair with a shifted frequency which creates a movable pattern of fringes, eliminating thus the ambiguity of the measurement. Each point has been analyzed for 90 s, capturing in the order of hundreds of particles. To validate the results, the particle has to be measured in both velocity components.

2.2.2 Laser-Doppler Vibrometry

For the LDV measurements, a Polytec PSV-500 scanning vibrometer has been used. The scanning has been performed through one of the lateral walls to measure the outermost fin, analyzing the perpendicular displacement field of the complete surface without the mass addition that accelerometers require. The LDV head was placed 1.5 m away from the fin, performing a grid discretization with a spatial resolution of 2.5 mm. Displacements in the order of picometers can be achieved by means of interpolation and demodulation techniques incorporated in the LDV. Measurements considered a bandwidth from 0 to 12.5 kHz with a frequency resolution lower than 1 Hz. The sampling frequency was set to 31.25 kHz and the final result is realized averaging 5 times the measured displacement.

2.2.3 Intrusive probes

The test section can also be equipped with accesses for intrusive instrumentation such as Pitot, Kiel, and 5-hole probes. Three automated XY gantries allow pre-programmed sweeps of the desired cross-sections. However, as stated in the introduction, reduced scale wind-tunnels can be particularly sensitive to intrusions. To measure the pressure drop, two piezometric rings with eight wall-flush tappings each are positioned up- and downstream of the test section, but the insertion of the probes will disturb these measurements, so these can only be performed in the optical configuration.

2.2.4 Thermal measurement & overall performance

Regarding the thermal characterization, a FLIR A400 thermographic camera has been used to determine the SACOC base temperature. It has been configured in the range from 0^oC to 120^oC with an accuracy of $\pm 2^oC$ and a resolution of 320 $\times$ 240 pixels. The Nusselt number associated with the heat exchanger under nominal conditions can be derived with this information. In this type of setup, specific windows transparent to long-wave infrared were used. On the oil side, heat transfer has been characterized by measuring the inlet-outlet temperature difference and the oil mass flow. To this end, eight Resistance Temperature Detectors (RTDs), half of them in the inlet and the other half in the outlet, have been placed beneath the SACOC to determine the temperature difference and the oil conditioning system Coriolis mass flow meter has been used to obtain the oil mass flow. In order to insulate the heat release and ensure that the heat transfer is produced only through the SACOC, the exchanger has been mounted in a 3D printed ULTEM 1010 thermoplastic oil pan. To obtain a baseline result, heat transfer and pressure drop were measured also substituting the finned SACOC with a flat one on the air side, preserving the oil-side geometry.

3. Results

In this section, the results obtained during the experimental characterization are presented. In the first place, the aerodynamic results show the velocity field captured during the experimental characterization by means of different techniques, as well as a vibration analysis of the outermost fin and the resulting Fanning friction coefficient. Then, thermal results are displayed and parameters such as the overall heat transfer coefficient and the Nusselt number are derived.

3.1 Aerodynamic characterization

Aerodynamic measurements in three different sections, one upstream (Plane 1) and two downstream (Planes 2 & 3) of the heat exchanger have been performed, demonstrating how velocity profiles measured along the vertical centerline are validated by means of intrusive measurements with Kiel total pressure probes. These results are presented in Fig. 3.

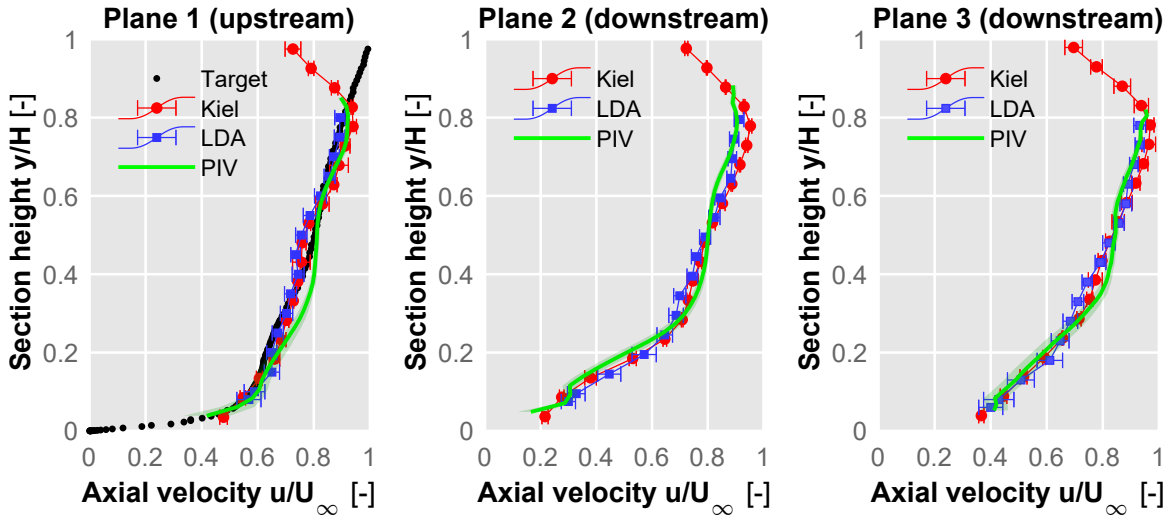

Figure 3 – Dimensionless central velocity profiles upstream (Plane 1) and downstream (Plane 2 & Plane 3) the heat exchanger comparing intrusive results (Kiel) and optical results (LDA & PIV).

In Plane 1, the velocity profile measured can be compared against the target velocity profile found in the turbofan bypass [5], confirming a good match for almost the complete height. In the downstream sections, it is possible to appreciate the aerodynamic deficit that appears in the fins' wake, stronger the closer to the exchanger, as well as how the flow remains almost unperturbed above the fins' height ($y/H = 0.2$), confirming the advantage of a reduced-height wind tunnel and the validity of the approach. In general, measurements carried out with different techniques present very similar values across the height of the tunnel, laying in most cases within the deviation of each measurement (indicated in Fig. 3 with error bars), and thereby cross-validating the different measurement techniques.

Once the results are validated, one of the advantages of the optical techniques, especially in the case of PIV, is the possibility of characterizing not only the centerline but the complete volume of the test section. Following a procedure such as the one presented in Fig. 4, measurements can be performed in different slices of the test section simply by moving the laser sheet.

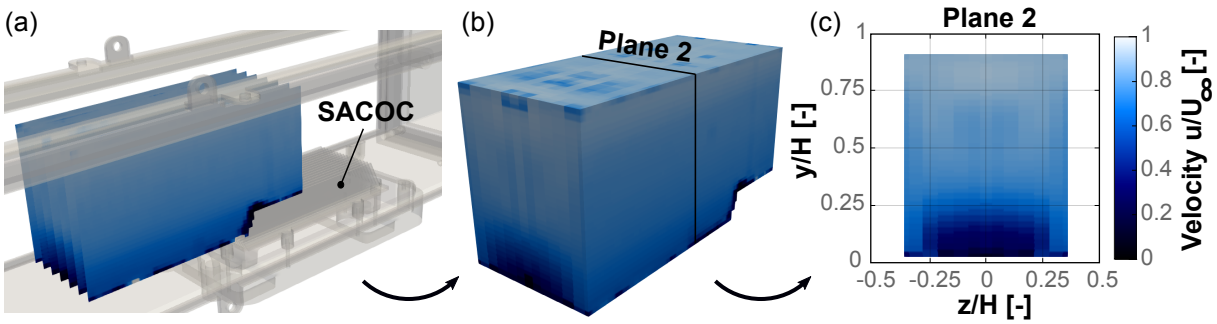

Figure 4 – Velocity analysis using PIV. (a) Experimental characterization of several planes. (b) Interpolation of the measurements to generate a volume. (c) Extraction of regions of interest.

In postprocessing, the obtained results can be interpolated to generate a volume containing the experimental data, from where any desired region of interest can then be extracted. For instance, Fig. 4 (c) shows the velocity distribution in Plane 2, downstream of the heat exchanger. The wake can be clearly noticed in this plane, showing how the side walls of the test section remain unperturbed by the velocity reduction downstream the SACOC.

While PIV is able to capture a snapshot of the whole flow field in its region of interest, the windowing of the data often precludes the characterization of precise points in the flow field. The LDA technique on the other hand, while only capable of measuring one point at a time, can extract data from a very precise location. In this way, it is analogous to a non-intrusive hot wire anemometer. Similarly, its high-frequency capabilities allow the characterization of highly dynamic flow features such as the turbulence intensity. Fig. 5 shows the TKI contours in the three defined measurement planes. The SACOC fins have been added to the representation to better understand the results. Note that only one half of the planes were measured to save time, the data then being mirrored on the other half.

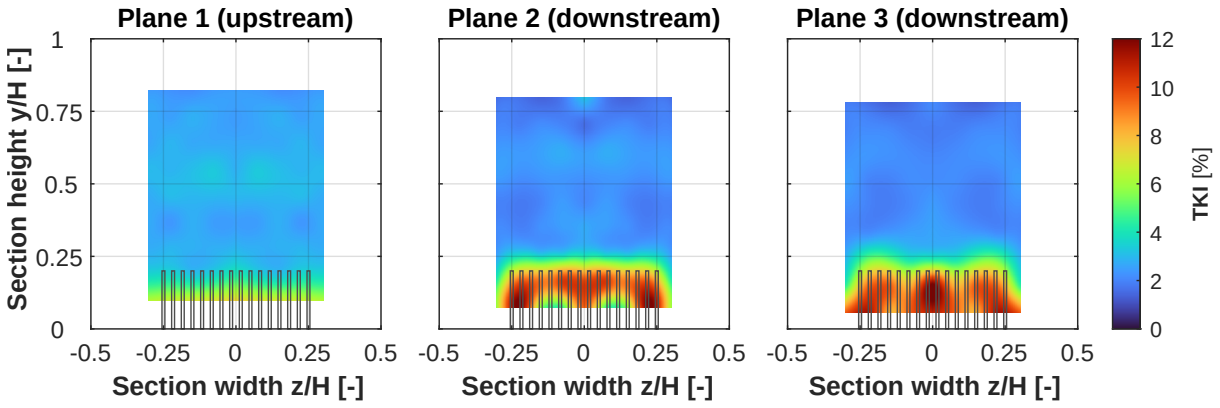

Figure 5 – Turbulent Kinetic Intensity measured with the LDA in the three planes of interest.

In the freestream region, values remain practically constant at around 2-3%. In Plane 1 it is possible to observe how the turbulence increases towards the bottom. This is caused by the presence of the distortion panel upstream, which presents lower porosity (smaller pores) in this region, causing not only a velocity reduction but a turbulence rise up to approximately 7%. This however is in line with the turbulence levels found in the engine bypass. Downstream the SACOC, in Planes 2 & 3, the wake is perfectly visible in terms of turbulence too. Its effect is relegated to a height slightly larger than the fins themselves and remains with similar values around 10% as further downstream.

3.2 Fluid-structure interaction

Another important characterization related to the aerodynamic performance is the vibration analysis of the SACOC. The averaged vibration spectrum of the outermost fin is shown in Fig. 6, together with the operational deflection shapes (ODSs) at selected frequencies, revealing the resonance modes of the heat exchanger excited by the flow field at nominal conditions.

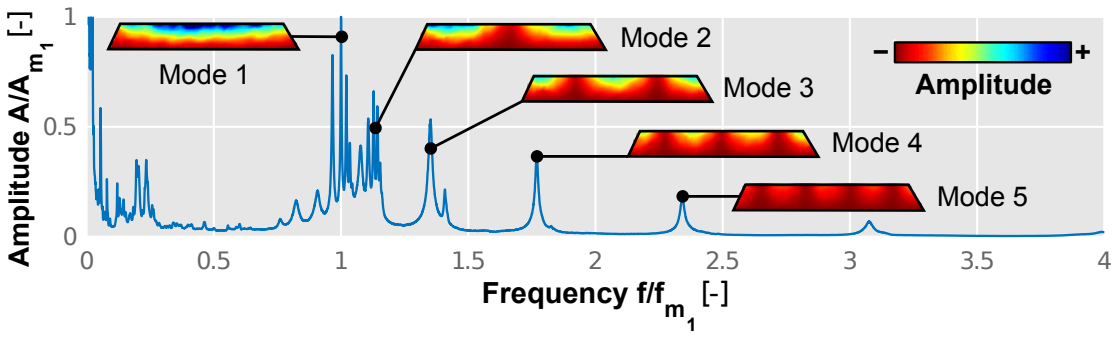

Figure 6 – Average vibration spectrum of the outermost fin and operational deflection shapes. Amplitudes and frequencies are rendered dimensionless with the values of the first mode.

It can be observed how the first modes show significant values of amplitude, whereas beyond the fourth mode, the amplitude barely reaches 20% of the first one. This experimental data is useful to validate finite element models (FEM) of the SACOC, which can be used to predict the resonance modes of the heat exchanger according to the fin geometry.

3.3 Thermal behavior

As for the thermal measurements, IR results are shown in Fig. 7. On the left-hand side, the temperature distribution is depicted. As expected, the tip of the fins presents lower values than the base, which in turn is cooler near the leading edge of the fins as it is further from the oil inlet and receives cooler air. The right-hand side of Fig. 7 shows the evolution of the temperature along lines perpendicular to the flow direction at three different percentages (25%, 50%, and 75%) of the fins' span, showing more clearly the temperature of the individual fins and highlighting the increased cooling of the outer fins. For these measurements, black graphite-based paint was applied to both the tunnel floor and heat exchanger, in order to obtain a uniform emissivity, which was calibrated through a thermocouple.

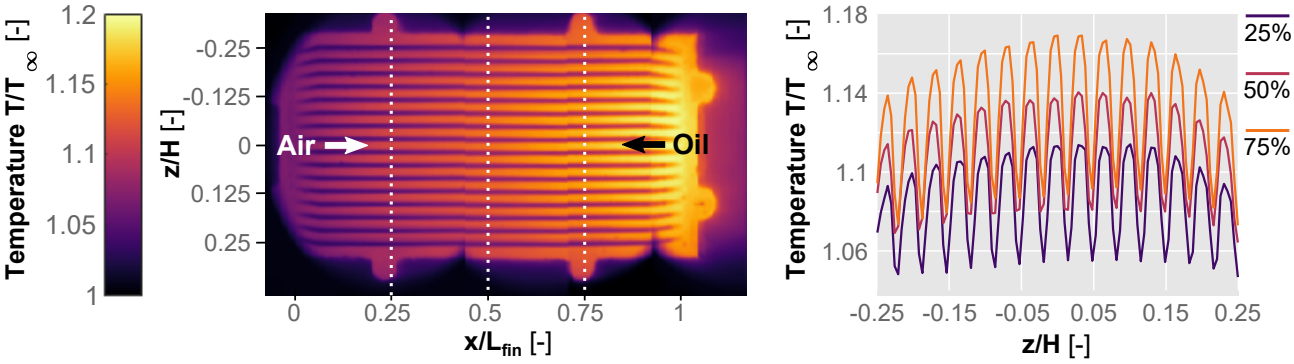

Figure 7 – On the left, dimensionless temperature distribution on the heat exchanger measured with IR thermography. On the right, temperatures along 25%, 50% and 75% of the fins length.

Extracting the base temperature data from the thermographic measurements and computing the heat transfer measured in the oil by means of the RTDs and mass flow meter, an approach similar to Tang et al. [13] and Incropera et al. [14] can be followed. Thermal parameters such as the overall heat transfer coefficient U or the film coefficient h can be computed and the Nusselt number ($Nu = hL/k$, where h is the film coefficient, L the length of the fins on the base, and k the air thermal conductivity) can be immediately derived.

After adding fins to the flat baseline SACOC, the heat transfer increased a 171.1%. A more representative value, that accounts for slight variations in inlet temperatures and mass flows, is the overall heat transfer coefficient, U which can be understood as the capacity of the SACOC to exchange heat between the working fluids. In the finned version, the U rises a 185.3% compared to the flat plate.
Considering the same characteristic length and the same conductivity for both cases, variations in the Nu come exclusively from the film coefficient h. In this case, the overall reduction between versions of the Nu number is 40%. It should be noted that this value is influenced by the surface available to exchange heat which, in the case of the finned version, is more than 10 times the area available in the baseline flat plate.

3.4 Overall performance

The advantage of using the reference flat plate to perform the characterization is that the overall performance results can be referred to this baseline, in order to properly isolate the effect of adding the fins on the air side of the bypass heat exchanger. The results at nominal operating conditions can be seen in Table 1, demonstrating how the finned version of the SACOC greatly increased the heat exchange, although the larger wet area lowered the Nusselt number and increased the pressure drop, expressed through the Fanning friction factor f.

Table 1 – Variation of the finned SACOC performance parameters against the flat-plate baseline.

$\Delta\dot{Q}$ [-]	ΔU [-]	ΔNu [-]	Δf [-]
171.1%	185.3%	-40%	191.7%

This pressure drop Δp across the test section is measured by a differential pressure sensor connected to the two piezometric rings shown in Fig. 1, and from it, the Fanning friction factor ($f = (\Delta p D_h)/(2Lv^2\rho)$, where D_h is the hydraulic diameter, v the mean velocity and ρ the density) can be computed. For high Reynolds numbers, such as in this investigation with Re in the order of $\sim 7.2\times10^6$, f values remain almost constant with variations in mass flow. Comparing the result obtained for the finned SACOC with that of the reference flat plate, the Fanning friction coefficient experiments an increase of 191.7%, highlighting the utmost importance of the proper aerodynamic design of SACOCs.

4. Conclusions

Non-intrusive techniques have been successfully applied to determine the performance of turbofan surface heat exchangers in a new reduced-scale facility, thus facilitating the development and validation of a key cooling technology for future aeroengines. The aerodynamic performance has been evaluated, employing different techniques, both optical and intrusive, to cross-validate the results.
We have shown how non-intrusive aerodynamic data can be exploited by reconstructing a volumetric flow field in the test section in order to characterize the SACOC wake in terms of size, turbulent intensity, etc. In this way, we have demonstrated that the influence of the SACOC wake is limited, and does not reach the upper or the lateral walls of the wind tunnel.
Furthermore, a preliminary fluid-structure interaction (FSI) study has been presented, revealing the amplitudes and frequencies of vibration in the outermost fin captured with a scanning laser-Doppler vibrometer, which is able to resolve the operating deflection shapes under nominal flow conditions and therefore easily validate FEM or even full FSI numerical simulations.
Finally, thermal and heat transfer measurements have been carried out, performing IR thermography to characterize the temperature distribution over the SACOC. By measuring the heat released by the oil circuit, the overall performance of the heat exchanger has been characterized, being compared against a baseline flat plate exchanger also taking pressure drop into account.
In summary, we have shown that a very complete aerothermal characterization of bypass heat exchangers for turbofan aeroengines can be reliably performed in a reduced-size wind tunnel exclusively through non-intrusive techniques, therefore greatly lowering the costs, times and environmental impacts of SACOCs development compared with full-size turbofan engine tests.

5. Contact author email address

Please address all correspondence to Jorge García-Tíscar at jorgarti@mot.upv.es (+34963877650).

6. Acknowledgements

This project has received funding from the Clean Sky 2 Joint Undertaking under the European Union's Horizon 2020 research and innovation programme under grant agreement nº 831977: *Aerodynamic upgrade of Surface Air-Cooled Oil Coolers (SACOC)*. A. Felgueroso is supported through the Programa de Apoyo para la Investigación y Desarrollo of the Universitat Politècnica de València under grant PAID-01-20 nº 21589. The authors also wish to acknowledge Mr. Adolfo Guzmán for his inestimable support during the experimental campaign.

7. Copyright statement

References

[1] Hart K. Basic Architecture and Sizing of Commercial Aircraft Gas Turbine Oil Feed Systems. *ASME Turbo Expo 2008: Power for Land, Sea, and Air*, Vol. 4: Heat Transfer, Parts A and B, pp 1431–1441, 2008.

[2] Gloeckner P and Rodway C. The Evolution of Reliability and Efficiency of Aerospace Bearing Systems. *Engineering*, Vol. 09, pp 962–991, 2017.

[3] Van Heerden A, Judt D, Lawson C, Jafari S, Nikolaidis T and Bosak D. Framework for integrated dynamic thermal simulation of future civil transport aircraft. *AIAA Scitech 2020 Forum*, American Institute of Aeronautics and Astronautics, 2020.

[4] Vankan W, Maas R and Peyron V. Optimisation methodology for integrated equipment installation in new engine architecture nacelles. *Proceedings of the Institution of Mechanical Engineers, Part G: Journal of Aerospace Engineering*, 2019.

[5] Broatch A, Olmeda P, García-Tíscar J, Felgueroso A, Chávez-Modena M, González L, Gelain M, and Couilleaux A. Experimental aerothermal characterization of surface air-cooled oil coolers for turbofan engines. *International Journal of Heat and Mass Transfer*, Vol. 190, pp 122775, 2022.

[6] Wen J, Li Y, Wang S and Zhou A. Experimental investigation of header configuration improvement in plate-fin heat exchanger. *Applied Thermal Engineering*, Vol. 27, pp 1761–1770, 2007.

[7] Yataghene M, Francine F and Jacl L. Flow patterns analysis using experimental PIV technique inside scraped surface heat exchanger in continuous flow condition. *Applied Thermal Engineering*, Vol. 31, pp 2855–2868, 2011.

[8] Scrittore J, Thole K and Burd S. Experimental Characterization of Film-Cooling Effectiveness Near Combustor Dilution Holes. *Proceedings of the ASME Turbo Expo*, Vol. 3, 2005.

[9] Buresti G, Talamelli A and Petagna P. Experimental characterization of the velocity field of a coaxial jet configuration. *Experimental Thermal and Fluid Science*, Vol. 9, pp 135–146, 1994.

[10] Ricci R, Romagnoli R, Montelpare S and Benedetto D. Convective heat transfer increase in internal laminar flow using a vibrating surface. *International Journal of Thermal Sciences*, Vol. 84, pp 358–368, 2014.

[11] Leblay P, Henry J, Caron D, Leducq D, Fournaison L and Bontemps A. Characterisation of the hydraulic maldistribution in a heat exchanger by local measurement of convective heat transfer coefficients using infrared thermography. *Energy Economics*, Vol. 45, pp 73–82, 2014.

[12] Mobtil M, Bougeard D and Russeil S. Experimental study of inverse identification of unsteady heat transfer coefficient in a fin and tube heat exchanger assembly. *International Journal of Heat and Mass Transfer*, Vol. 125, pp 17–31, 2018.

[13] Tang L, Zeng M and Wang Q. Experimental and numerical investigation on air-side performance of fin-and-tube heat exchangers with various fin patterns. *Experimental Thermal and Fluid Science*, Vol. 33, pp 818–827, 2009.

[14] Incropera F, DeWitt D, Bergman T and Lavine A. *Fundamentals of Heat and Mass Transfer*. 6th edition, John Wiley and Sons Ltd, 2010.